

CrystEngComm

Accepted Manuscript



This is an *Accepted Manuscript*, which has been through the Royal Society of Chemistry peer review process and has been accepted for publication.

Accepted Manuscripts are published online shortly after acceptance, before technical editing, formatting and proof reading. Using this free service, authors can make their results available to the community, in citable form, before we publish the edited article. We will replace this *Accepted Manuscript* with the edited and formatted *Advance Article* as soon as it is available.

You can find more information about *Accepted Manuscripts* in the [Information for Authors](#).

Please note that technical editing may introduce minor changes to the text and/or graphics, which may alter content. The journal's standard [Terms & Conditions](#) and the [Ethical guidelines](#) still apply. In no event shall the Royal Society of Chemistry be held responsible for any errors or omissions in this *Accepted Manuscript* or any consequences arising from the use of any information it contains.



Graphene oxide templated preferential growth of continuous MOF thin films

Received 00th January 20xx,
Accepted 00th January 20xx

Daeok Kim,^a Ali Coskun^{a,b*}

DOI: 10.1039/x0xx00000x

www.rsc.org/

We introduced a new strategy to fabricate defect-free continuous metal-organic framework (MOF) films using graphene oxide (GO) as an interfacial template on solid substrates. Unprecedented formation of one-dimensional nanorod-shaped crystalline intermediate phase on the GO surface enabled preferential growth of HKUST-1 film in the <220> direction.

Metal-organic frameworks (MOFs) are highly porous crystalline materials with tunable pore characteristics, which are easily tailored by the combinational choice of various metals and organic ligands.¹ Intrinsic features of MOFs such as high surface area, well-defined pore size and high metal density have expanded their applications to gas storage/separation,²⁻⁴ heterogeneous catalyst,^{5,6} sensor,⁷ semiconductor,⁸ energy storage^{9,10} applications. In particular, thin film coating of MOFs onto substrates has potential to pave the way for various applications such as luminescence, catalysis, gas separation (membrane), sensor and other nano-devices by introducing new properties that are not available in the solid powder form.¹¹⁻¹³ In the MOF film development, however, immobilization of well-grown continuous MOF films onto various substrates has been a significant challenge, thus various growth procedures such as direct growth on functionalized substrate,¹⁴⁻¹⁶ layer-by-layer,¹⁷ liquid phase epitaxial growth,¹⁸ seeding- secondary growth,¹⁹⁻²² chemical solution deposition,²³ electrochemical synthesis^{24,25} and microwave-assisted method^{26,27} have been developed. Among these techniques, seeding-hydrothermal secondary growth is widely adopted method for the fabrication of MOF thin films, in which it is crucial to achieve uniformly dispersed and strongly bounded seeding on the substrate to form a continuous well-grown film. To date, several seeding techniques such as microwave-assisted,¹⁹ thermal heating,²⁰

reactive seeding,²¹ step by step,²⁸ and rubbing²⁹ have been proposed, however, there is still a significant challenge restricting their application, that is the dependency of seeding procedure on the types of substrate. Moreover, the formation of defect-free MOF films is still an important problem for their application as gas separation membranes.

Graphene oxide (GO) as a two-dimensional macromolecule offers unique advantages such as rich surface chemistry through oxygen functionalities, ability to form free-standing films and ease of fabrication on any kind of substrate including porous substrates and electrodes.^{30,31} For the preparation of MOF membranes, oxygen functionalities located on the surface of GO can offer strong bonding/adhesion for the MOF seed crystals and thus eventually template the formation of continuous MOF films on various substrates. In addition, the resulting composite membrane could inherit some of the unique features of GO such as ultramolecular sieving effect^{32,33} and electronic properties.³⁴ Herein, we demonstrated that GO film can be used as an interfacial template for the MOF seeding and subsequent growth of continuous MOF films on HKUST-1³⁵ *via* thermal seeding and its secondary growth on the anionic alumina oxide (AAO) film. We have also observed preferential MOF crystal growth in the <220> direction on the GO film, thus providing us with a unique tool to control pore aperture for the gas separation applications.

The synthesis of GO was achieved (see synthesis section for details, ESI) using modified Hummers' method.³⁶ For the preparation of GO films, porous AAO film with ~200 nm of pore size was used (Fig. 1a) as a substrate. AAO not only have high thermal and chemical stability under our experimental conditions, but it also allowed us to prepare GO films with a few-nanometer thickness *via* simple, vacuum-assisted layer by layer assembly procedure in H₂O at room temperature.³³ In order to prepare the GO film, 1.5 mL of dispersed GO solution (0.025 mg mL⁻¹) was poured onto the AAO substrate and as vacuum applied on the opposite side of AAO film, the amount of solvent was reduced gradually, thus leading to the formation of a layered GO sheet (Fig. 1b). The resulting GO film

^a Graduate school of EEWS, Korea Advanced Institute of Science and Technology (KAIST), 291 Daehak-ro, Yuseong-gu, Daejeon, 305-701, Republic of Korea.

^b Department of Chemistry, Korea Advanced Institute of Science and Technology (KAIST), Daejeon 305-701, Republic of Korea.

† Electronic Supplementary Information (ESI) available: Materials and experimental methods, FTIR, XRD, XPS, Digital images. See DOI: 10.1039/x0xx00000x

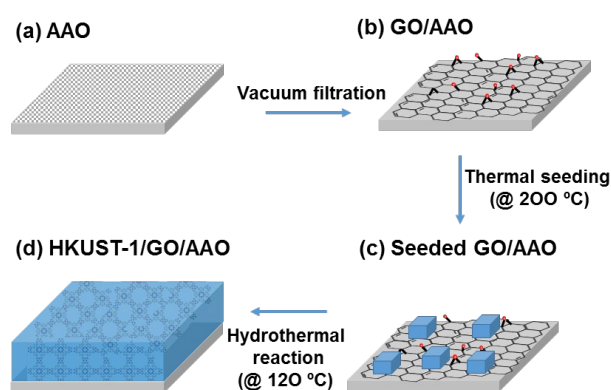


Fig. 1 Schematic description of HKUST-1 film growth on the GO film located on anionic alumina oxide (AAO) substrate.

on the AAO substrate (GO/AAO) was placed in 200°C oven for 15 min, after which pre-synthesized HKUST-1 seed solution was added (Fig. 1c) and kept for 20 min. After EtOH washing and subsequent drying steps, the seeded GO/MOF was placed in a reactor containing the solution of MOF precursors and kept at 120°C for 6 h for the synthesis of continuous HKUST-1 film (Fig. 1d).

In order to monitor the structural and chemical changes during formation of HKUST-1 film, we have carried out scanning electron microscopy (SEM) and Fourier transform infrared spectroscopy (FT-IR) analyses. SEM (Fig. 2a) and FT-IR (Fig. 2d) analyses of AAO and GO/AAO indicate the successful fabrication of GO film on the AAO substrate. Importantly, GO film covered completely all the pores and surface of AAO, thus creating a functional surface containing rich oxygen functionalities such as epoxide, hydroxyl and carboxylic acid. After seeding, we observed (Fig. 2b) a few tenths of a nanometer of HKUST-1 nanocrystals attached onto the GO surface along with an unusual nanorod-shaped phase, which could be attributed to the formation of aggregated one-dimensional (1D) polymer chains composed of trimesic acid (TMA) and Cu(II) ions. Although, FT-IR analysis of the seeded GO/AAO showed similar peaks to those of HKUST-1, XRD measurement revealed (Fig. 2e) completely different crystalline phase for the nanorods. After subsequent hydrothermal reaction, however, these nanorods fully transformed into HKUST-1 film containing micron-sized intergrown crystals (Fig. 2c). XRD analysis of the film revealed high crystallinity of the synthesized HKUST-1 film (Fig. 2e).

In order to understand the formation mechanism of HKUST-1 film on the GO surface, we have carried out detailed chemical and structural analysis. Firstly, we investigated the structural changes of GO film at 200°C (at the seeding temperature). C1s X-ray Photoelectron Spectroscopy (XPS) analysis of GO/AAO revealed two sharp and a weak shoulder peak at 284, 286 and 288 eV, indicating C-C, C-O and C=O bonds, respectively.³⁷ The intensity of C-O peak decreased (see Fig. S1, ESI) significantly following the thermal treatment at 200°C. In addition, FT-IR analysis showed noticeable decrease

of a broad peak in the range 3038-3490 cm^{-1} region, indicating the disappearance of intercalated water and -OH functional groups (see Fig. S2a, ESI). In addition, we have also observed a shift of GO (001) diffraction peak from 10.6 to 8.2 degree in the XRD spectrum, indicating the expansion of interlayer d spacing from 8.3 to 10.9 Å (see Fig. S2b, ESI). As the thermal treatment of GO layers can lead to partial graphenization, the formation of CO and CO₂ gases during the reduction process and the removal of water molecules might induce the expansion GO layers.³⁸ Although the heat treatment process significantly reduced the number of functional groups on the GO surface, the remaining functional groups could still act as anchors for the HKUST-1 seed crystals by coordinating to the Cu²⁺ centers. It is important to note that any physisorbed seed crystals would be removed during the post-washing step, thus the seed crystals remained on the surface should be chemically attached to the GO surface. Such interaction was also observed by Guerrero *et al.*,²⁰ they have shown that both organic linkers and Cu species (Cu²⁺ and Cu(II) paddle-wheel complex) serve as binders to form strong connection between HKUST-1 crystals and AAO substrate.

In order to examine how HKUST-1 seed crystals attach onto the thermally treated GO/AAO, we have prepared four control seed solutions containing HKUST-1 seed crystals, namely EtOH/H₂O/Cu/TMA, EtOH/H₂O/Cu, EtOH/H₂O/TMA and EtOH/H₂O. Each solution was seeded (see Fig. S3, ESI) onto GO/AAO substrates at 200°C. We have only observed corresponding XRD peaks for the HKUST-1 (see Fig. S4) in the case of EtOH/H₂O/Cu/TMA seed solution, indicating that either TMA or Cu²⁺ can't connect MOF crystals to GO surface and both TMA and Cu²⁺ are required for the stable and successful seeding of HKUST-1 crystals onto the GO/AAO film.²⁰ Surprisingly, we have also observed an unusual crystalline phase in the form of nanorods during the seeding procedure. In order to understand the origin of this new crystalline phase we have carried out XRD analyses for the seed crystals collected by centrifuging the seed solution at room temperature and also for the GO/AAO films seeded at 120 and 200°C (see Fig. S5, ESI). Evidently, the formation of new crystalline phase was only observed after seeding at high temperatures such as 120 and 200°C, indicating that the new phase did not originate from the seed crystals, but formed during the seeding process at high temperature. Considering the stability of HKUST-1 crystals under the seeding condition, the MOF precursors (TMA and Cu²⁺) remained unreacted in the seed solution could lead to the formation of crystalline rod-like superstructures on the GO surface. In order to further support our hypothesis, we prepared mixture of HKUST-1 precursors to have the same Cu²⁺ and TMA concentrations as the seed solution and carried out seeding experiment on the GO/AAO substrate. XRD analysis revealed (see Fig. S6, ESI) the formation of the same crystalline phase, thus proving the fact that the formation of rod-like superstructures originate from unreacted HKUST-1 precursors in the seed solution.

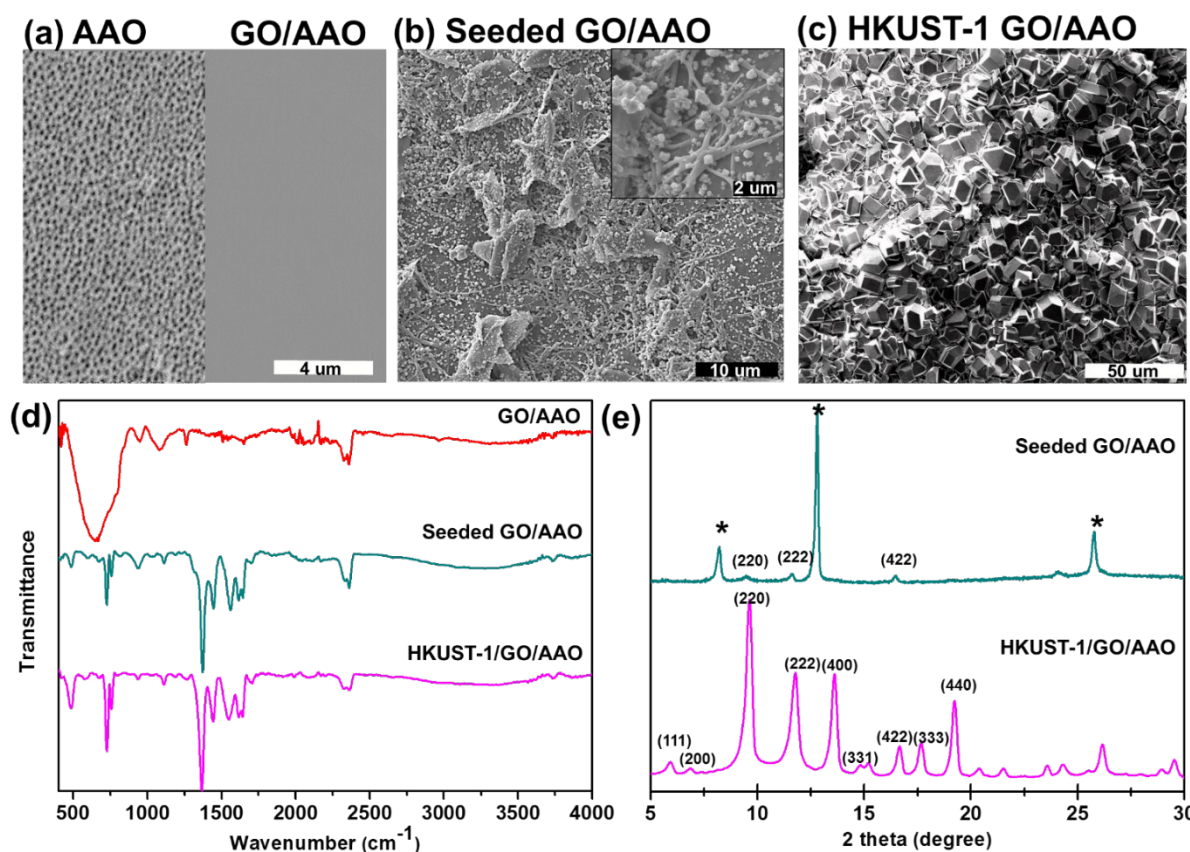


Fig. 2 Fabrication of HKUST-1 film on the GO/AAO substrate and its characterization. SEM images of (a) AAO and GO/AAO, (b) Seeded GO/AAO and (c) HKUST-1/GO/AAO, respectively; inset in (b) is an enlarged view. (d) FT-IR and (e) XRD data during the consecutive seeding and hydrothermal reactions.

In order to analyze the electronic state of Cu in the rod-like nanostructures, we have carried out Cu 2P XPS measurement. We have observed (see Fig. S7, ESI) only Cu^{2+} species in the XPS spectrum, just like HKUST-1. The similarity of XPS and FT-IR results between seeded GO/AAO and HKUST-1 indicates that the new crystalline phase has similar chemical structure to that of HKUST-1 originating from the connection of Cu^{2+} and TMA. More importantly, this rod-like crystalline phase completely disappeared and transformed (see Fig. 2e) into HKUST-1 after hydrothermal reaction.

HKUST-1 film grown on the seeded GO/AAO showed two distinctive features/advantages compared to the one grown on the bare AAO substrate: 1) formation of uniform, defect-free and continuous films even after one seeding cycle and 2) preferential growth of HKUST-1 crystals. In order to demonstrate the impact of GO-templation on the HKUST-1 film formation, we have grown HKUST-1 films on bare AAO (HKUST-1/AAO) using the same procedure to that of GO/AAO. The resulting film was analyzed by SEM (Fig. 3a) and XRD (Fig. 3c). SEM analysis of HKUST-1/AAO revealed MOF nanocrystals ($\sim 6 \mu\text{m}$) attached onto the AAO surface without the formation of a continuous film. We attribute this result to the fact that strong and evenly dispersed seeding was not achieved due to the large pore size ($\sim 200 \text{ nm}$) and small exposed surface of AAO for the connection with seed crystals. On the contrary, HKUST-1/GO/AAO showed continuous film structure formed

by the intergrown HKUST-1 nanocrystals ($\sim 11 \mu\text{m}$). These results clearly demonstrate the impact of GO-templation for the formation of continuous MOF films even after one seeding cycle. It is important to note that bare AAO film requires multiple seeding cycles.²⁰ In order to further verify the effect of GO on the seeding and film growth, partially exfoliated GO/AAO substrate, in which GO-free regions were intentionally created on the AAO surface *via* sonicating GO/AAO for 10 min, was prepared. Following the seeding and hydrothermal growth steps, while we only observed (see Fig. S8, ESI) formation of MOF crystals on the GO, GO-free AAC surface remained bare. In order to compare the thickness of films, we have recorded cross-sectional images of HKUST-1/AAO (Fig. 3a) and HKUST-1/GO/AAO (Fig. 3b) films, wherein thick smooth layers (below) and rough layers (above) correspond to AAO and HKUST-1 films, respectively. We have observed significant difference in film thickness for HKUST-1/AAO ($\sim 6 \mu\text{m}$) and HKUST-1/GO/AAO ($\sim 52 \mu\text{m}$). The lower thickness in the case of HKUST-1/AAO indicates the existence of dispersed HKUST-1 nanocrystals attached to the AAO surface. However, the thickness of well-intergrown HKUST-1 film on the GO/AAO substrate was almost five times of a single nanocrystal ($\sim 11 \mu\text{m}$) on the GO surface. This result indicates the successive growth on the surface of both pre-grown MOF and the GO as both the surface of MOF seed crystals and GO can act as nucleation sites for the MOF crystallization.

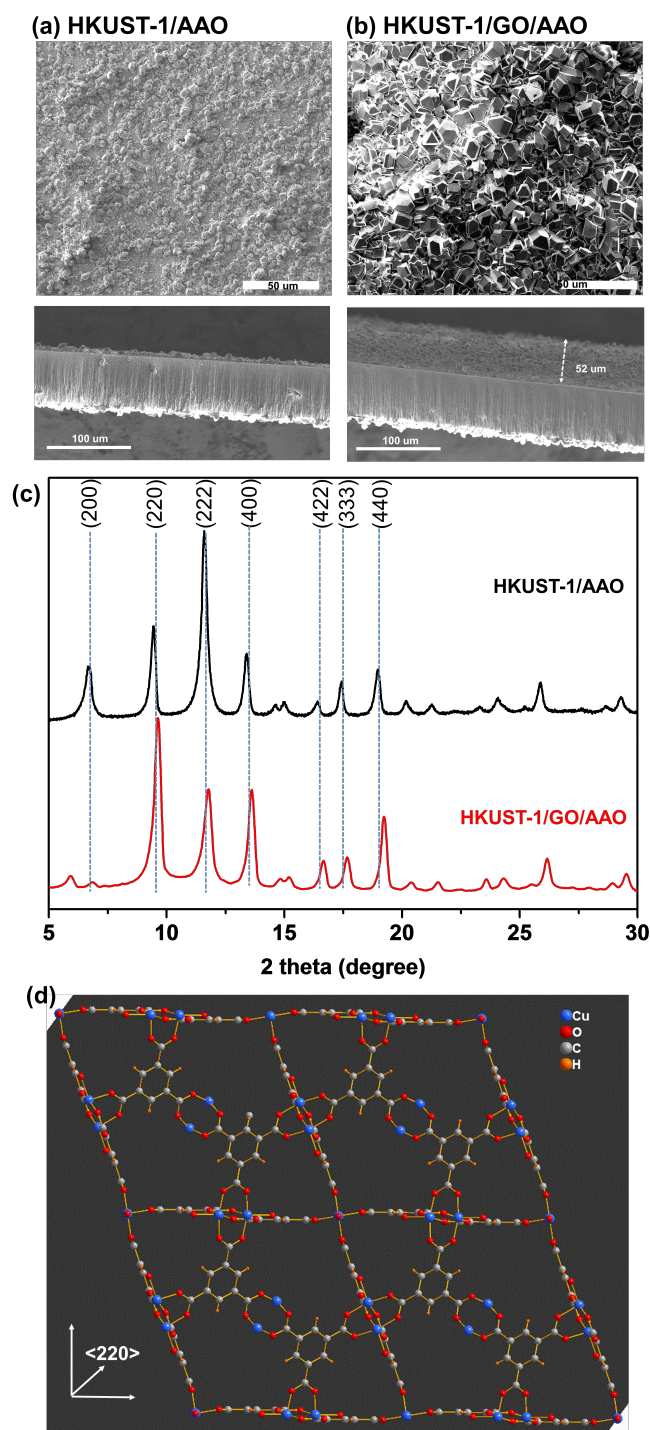


Fig. 3 Structural analysis for the influence of GO film on the growth of HKUST-1. SEM images of HKUST-1 fabricated on (a) AAO and (b) GO/AAO substrates. Top (above) and cross-sectional (below) views. c) XRD spectra of HKUST-1/AAO and HKUST-1/GO/AAO samples. d) The crystal structure of HKUST-1 viewed along the $\langle 220 \rangle$ direction.

GO film also influenced the growth direction of HKUST-1 crystals, which is reflected (Fig. 3c) by the different peak intensity in the XRD spectra of HKUST-1/AAO and HKUST-1/GO/AAO. In the case of the former, XRD pattern followed that of HKUST-1 powder and exhibited (see Fig. S9, ESI) the highest intensity peak on the (222) plane, however, HKUST-

1/GO/AAO XRD spectrum revealed two noticeable differences (1) almost complete disappearance of (200) peak and (2) the highest peak intensity on the (220) plane. This result indicates the fact that GO can inhibit the growth of HKUST-1 in $\langle 200 \rangle$ and promote growth in $\langle 220 \rangle$ and $\langle 222 \rangle$ directions. Although, there have been results showing the preferential growth of HKUST-1 in the $\langle 111 \rangle$ and $\langle 100 \rangle$ directions under specifically controlled conditions such as COOH and OH functionalized self-assembled monolayers (SAMs)^{39,40} or using solid modulators,⁴¹ to the best of our knowledge, this is first demonstration of HKUST-1 crystal growth in the $\langle 220 \rangle$ direction. While the solid-modulators enabled the formation of continuous MOF films, they require complex preparation procedures. On the contrary, our method provides facile route to the preparation of continuous and preferentially oriented HKUST-1 film in the $\langle 220 \rangle$ direction.

In order to elucidate the origin of the GO-templated preferential growth of HKUST-1 on the GO surface, structural changes of HKUST-1 crystals during the seed preparation, seeding and hydrothermal reaction steps were analyzed. The XRD pattern of the seed crystal was found (see Fig. S5, ESI) to be similar to that of HKUST-1 except slight increase in (200) peak, indicating that the influence of HKUST-1 seed crystals or preferential growth of MOF film could be minimal. The XRD pattern after thermal seeding showed higher intensity peak in $\langle 222 \rangle$ direction compared to $\langle 220 \rangle$, however, without any preferential orientation in the $\langle 222 \rangle$ direction (Fig. 2e). The crystals precipitated in the MOF-growing reactor also revealed (see Fig. S10, ESI) similar XRD patterns to that of HKUST-1. Based on these findings, we concluded that the preferential growth was realized during hydrothermal reaction on the surface of GO, thus clearly demonstrating the importance of GO-templation. We speculate that the formation of aggregated one-dimensional (1D) polymer chains on the GO surface play a significant role for the preferential growth of MOF crystals on the GO surface. It is important to note that this new crystalline phase and preferential growth was not observed in the case of bare AAO film.²⁰ We believe that the transformation of these crystalline rod-like superstructures into HKUST-1 crystals on the GO surface leads to unique preferential growth of MOF crystals. Evidently, similar transformation of 1D coordination polymer into 3D MOF was also observed by Lee *et al.*⁴²

In summary, we have demonstrated that GO-templation approach can facilitate the fabrication of continuous HKUST-1 films on solid-substrates. In addition, the formation of rod-like crystalline intermediate phase on the GO surface enabled control over the growth direction of MOF crystals. These results signify the importance of substrate and the intermediate states in controlling the growth direction of crystals. Controlling the pore apertures of MOF films is particularly important to form selective membranes *via* molecular sieving for gas separation applications. We also believe that the GO-templation approach can be extended to various substrates to grow different MOF thin films as a universal strategy, thus extending the applications of MOF

films to membranes, sensors, electronic devices and light-harvesting systems.

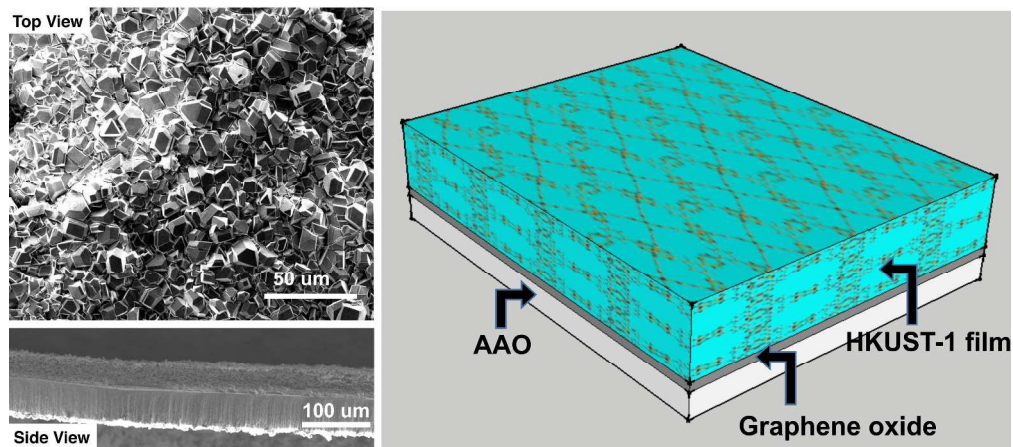
Acknowledgements

We acknowledge the support from the Basic Science Research Program through the National Research Foundation of Korea (NRF) funded by the Ministry of Science, ICT & Future Planning (2013R1A1A1012282). This work was also partially supported by the National Research Foundation of Korea (NRF) Grant funded by the Korea government (MEST) (NRF-2014R1A4A1003712).

Notes and references

- 1 T. H. Chen, I. Popov, W. Kaveevivitchai and O. S. Miljanic, *Chem. Mater.*, 2014, **26**, 4322-4325.
- 2 P. Bose, L. Y. Bai, R. Ganguly, R. Q. Zou and Y. L. Zhao, *Chempluschem*, 2015, **80**, 1259-1266.
- 3 J. R. Li, R. J. Kuppler and H. C. Zhou, *Chem. Soc. Rev.*, 2009, **38**, 1477-1504.
- 4 G. Srinivas, W. Travis, J. Ford, H. Wu, Z. X. Guo and T. Yildirim, *J. Mater. Chem. A*, 2013, **1**, 4167-4172.
- 5 J. Lee, O. K. Farha, J. Roberts, K. A. Scheidt, S. T. Nguyen and J. T. Hupp, *Chem. Soc. Rev.*, 2009, **38**, 1450-1459.
- 6 X. Yu and S. M. Cohen, *Chem. Comm.*, 2015, **51**, 9880-9883.
- 7 L. E. Kreno, K. Leong, O. K. Farha, M. Allendorf, R. P. Van Duyne and J. T. Hupp, *Chem. Rev.*, 2012, **112**, 1105-1125.
- 8 C. G. Silva, A. Corma and H. Garcia, *J. Mater. Chem.*, 2010, **20**, 3141-3156.
- 9 S. Y. Jin, H. J. Son, O. K. Farha, G. P. Wiederrecht and J. T. Hupp, *J. Am. Chem. Soc.*, 2013, **135**, 955-958.
- 10 C. Y. Lee, O. K. Farha, B. J. Hong, A. A. Sarjeant, S. T. Nguyen and J. T. Hupp, *J. Am. Chem. Soc.*, 2011, **133**, 15858-15861.
- 11 A. Betard and R. A. Fischer, *Chem. Rev.*, 2012, **112**, 1055-1083.
- 12 D. Bradshaw, A. Garai and J. Huo, *Chem. Soc. Rev.*, 2012, **41**, 2344-2381.
- 13 O. Shekhah, J. Liu, R. A. Fischer and C. Woll, *Chem. Soc. Rev.*, 2011, **40**, 1081-1106.
- 14 Z. S. Dou, J. C. Yu, H. Xu, Y. J. Cui, Y. Yang and G. D. Qian, *Thin Solid Films*, 2013, **544**, 296-300.
- 15 S. Hermes, F. Schroder, R. Chelmowski, C. Woll and R. A. Fischer, *J. Am. Chem. Soc.*, 2005, **127**, 13744-13745.
- 16 O. Kozachuk, K. Yussenko, H. Noei, Y. M. Wang, S. Walleck, T. Glaser and R. A. Fischer, *Chem. Comm.*, 2011, **47**, 8509-8511.
- 17 J. J. Zhao, B. Gong, W. T. Nunn, P. C. Lemaire, E. C. Stevens, F. I. Sidi, P. S. Williams, C. J. Oldham, H. J. Walls, S. D. Shepherd, M. A. Browe, G. W. Peterson, M. D. Losego and G. N. Parsons, *J. Mater. Chem. A*, 2015, **3**, 1458-1464.
- 18 B. Liu and R. A. Fischer, *Sci. China. Chem.*, 2011, **54**, 1851-1866.
- 19 Y. Yoo, Z. P. Lai and H. K. Jeong, *Micropor. Mesopor. Mater.*, 2009, **123**, 100-106.
- 20 V. V. Guerrero, Y. Yoo, M. C. McCarthy and H. K. Jeong, *J. Mater. Chem.*, 2010, **20**, 3938-3943.
- 21 Y. X. Hu, X. L. Dong, J. P. Nan, W. Q. Jin, X. M. Ren, N. P. Xu and Y. M. Lee, *Chem. Comm.*, 2011, **47**, 737-739.
- 22 Y. Y. Mao, W. Cao, J. W. Li, L. W. Sun and X. S. Peng, *Chem. Eur. J.*, 2013, **19**, 11883-11886.
- 23 J. L. Zhuang, D. Ceglarek, S. Pethuraj and A. Terfort, *Adv. Funct. Mater.*, 2011, **21**, 1442-1447.
- 24 T. R. C. Van Assche, G. Desmet, R. Ameloot, D. E. De Vos, H. Terryn and J. F. M. Denayer, *Micropor. Mesopor. Mater.*, 2012, **158**, 209-213.
- 25 B. Van de Voorde, R. Ameloot, I. Stassen, M. Everaert, D. De Vos and J. C. Tan, *J. Mater. Chem. C*, 2013, **1**, 7716-7724.
- 26 Z. Q. Li, M. Zhang, B. Liu, C. Y. Guo and M. Zhou, *Inorg. Chem. Comm.*, 2013, **36**, 241-244.
- 27 Y. Yoo and H. K. Jeong, *Chem. Comm.*, 2008, 2441-2443.
- 28 J. P. Nan, X. L. Dong, W. J. Wang, W. Q. Jin and N. P. Xu, *Langmuir*, 2011, **27**, 4309-4312.
- 29 S. Balakrishnan, A. J. Downard and S. G. Telfer, *J. Mater. Chem.*, 2011, **21**, 19207-19209.
- 30 D. A. Dikin, S. Stankovich, E. J. Zimney, R. D. Piner, G. H. B. Dommett, G. Evmenenko, S. T. Nguyen and R. S. Ruoff, *Nature*, 2007, **448**, 457-460.
- 31 H. Y. Jeong, J. Y. Kim, J. W. Kim, J. O. Hwang, J. E. Kim, J. Y. Lee, T. H. Yoon, B. J. Cho, S. O. Kim, R. S. Ruoff and S. Y. Choi, *Nano Lett.*, 2010, **10**, 4381-4386.
- 32 R. K. Joshi, P. Carbone, F. C. Wang, V. G. Kravets, Y. Su, I. V. Grigorieva, H. A. Wu, A. K. Geim and R. R. Nair, *Science*, 2014, **343**, 752-754.
- 33 H. Li, Z. N. Song, X. J. Zhang, Y. Huang, S. G. Li, Y. T. Mao, H. Ploehn, Y. Bao and M. Yu, *Science*, 2013, **342**, 95-98.
- 34 S. F. Pei and H. M. Cheng, *Carbon*, 2012, **50**, 3210-3228.
- 35 S. S. Y. Chui, S. M. F. Lo, J. P. H. Charmant, A. G. Orpen and I. D. Williams, *Science*, 1999, **283**, 1148-1150.
- 36 W. Hummers, R. Offeman, *J. Am. Chem. Soc.*, 1958, **80**, 1339-1339.
- 37 S. Stankovich, D. A. Dikin, R. D. Piner, K. A. Kohlhaas, A. Kleinhammes, Y. Jia, Y. Wu, S. T. Nguyen and R. S. Ruoff, *Carbon*, 2007, **45**, 1558-1565.
- 38 Y. Qiu, F. Guo, R. Hurt and I. Kulaots, *Carbon*, 2014, **72**, 215-223.
- 39 N. Nijem, K. Fursich, S. T. Kelly, C. Swain, S. R. Leone and M. K. Gilles, *Cryst. Growth Des.*, 2015, **15**, 2948-2957.
- 40 J. L. Zhuang, D. Ceglarek, S. Pethuraj and A. Terfort, *Adv. Funct. Mater.*, 2011, **21**, 1442-1447.
- 41 Y. Y. Mao, B. B. Su, W. Cao, J. W. Li, Y. L. Ying, W. Ying, Y. J. Hou, L. W. Sun and X. S. Peng, *ACS Appl. Mater. Inter.*, 2014, **6**, 15676-15685.
- 42 E.-Y. C. Seung-Chul Lee, Sang-Beom Lee, Sang-Wook Kim, O-Pil Kwon, *Chem. Eur. J.*, 2015, **21**, 15570-15574.

TOC text: Graphene oxide film was used as an interfacial template for the preferential growth of continuous HKUST-1 films on a solid-substrate.



430x195mm (300 x 300 DPI)